MODELING THE DYNAMICS OF SEDIMENT TRANSPORT, TIDES, AND SEA-LEVEL RISE: IMPLICATIONS FOR THE RESILIENCE OF COASTAL BENGAL

Christopher M. Tasich Jonathan M. Gilligan George M. Hornberger

Department of Civil and Environmental Engineering
Department of Earth and Environmental Sciences
Vanderbilt University
2301 Vanderbilt Place, PMB 351831
Nashville, TN 37235–1831, USA

ABSTRACT

The coastal zone of the Ganges-Brahmaputra-Meghna (GBM) Delta is widely recognized as one of the most vulnerable places to sea-level rise (SLR), with around 57 million people living within 5 m of sea level. Sediment transported by the Ganges, Brahmaputra, and Meghna rivers has the potential to raise the land and offset SLR. There is significant uncertainty in future sediment supply and SLR, which raises questions about the sustainability of the delta. We present a simple model, driven by basic physics, to estimate the evolution of the landscape under different conditions at low computational cost. Using a single tuning parameter, the model can match observed rates of land aggradation. We find a strong negative feedback, which robustly brings land elevation into equilibrium with changing sea level. We discuss how this model can be used to investigate the dynamics of sediment transport and the sustainability of the GBM Delta.

1 INTRODUCTION

Coastal Bengal is situated within the GBM Delta formed by the confluence of the Ganges, Brahmaputra, and Meghna rivers and straddles the border between West Bengal, India to the east and Bangladesh to the west. The region is home to around 57 million people and the ecologically critical Sundarbans mangrove forest. During the 1960s and 1970s, the Coastal Embankment Project (CEP) clear-cut large swaths of mangrove forest, and constructed extensive earthen embankments (locally known as "polders") to protect low-lying areas from flooding during high tides, storms, and monsoon rains. This effort reclaimed intertidal land and enabled agriculture and aquaculture year-round. However, the creation of polders significantly altered the region's natural geomorphic and tidal processes (Pethick and Orford 2013; Brammer 2014; Auerbach et al. 2015; Roy et al. 2017; Alam et al. 2017; Wilson et al. 2017; Bain et al. 2019; van Maren et al. 2023).

Further complicating this problem is the imminent threat of SLR to the region (Becker et al. 2020; Steckler et al. 2022). The delta is often portrayed as one of the most at-risk regions for SLR due to its vast expanse of low-lying land at or near sea level. Many studies (Sarwar 2005; Dasgupta et al. 2009; Loucks et al. 2010) suggest large swaths of the delta may be flooded under different SLR scenarios. However, this overly simplifies the threat to the region and neglects the significant sediment contribution of the GBM system in maintaining the natural elevation.

The role of sediment is especially important within the tide-dominated Sundarbans mangrove forest. Much of the Sundarbans are largely disconnected from the fluvial network and rely mostly on tidal reworking of sediment from the GBM river mouth. Recent work by Raff et al. (2023) demonstrates that sediment deposition may raise land elevation at a comparable rate to SLR, especially if global warming intensifies

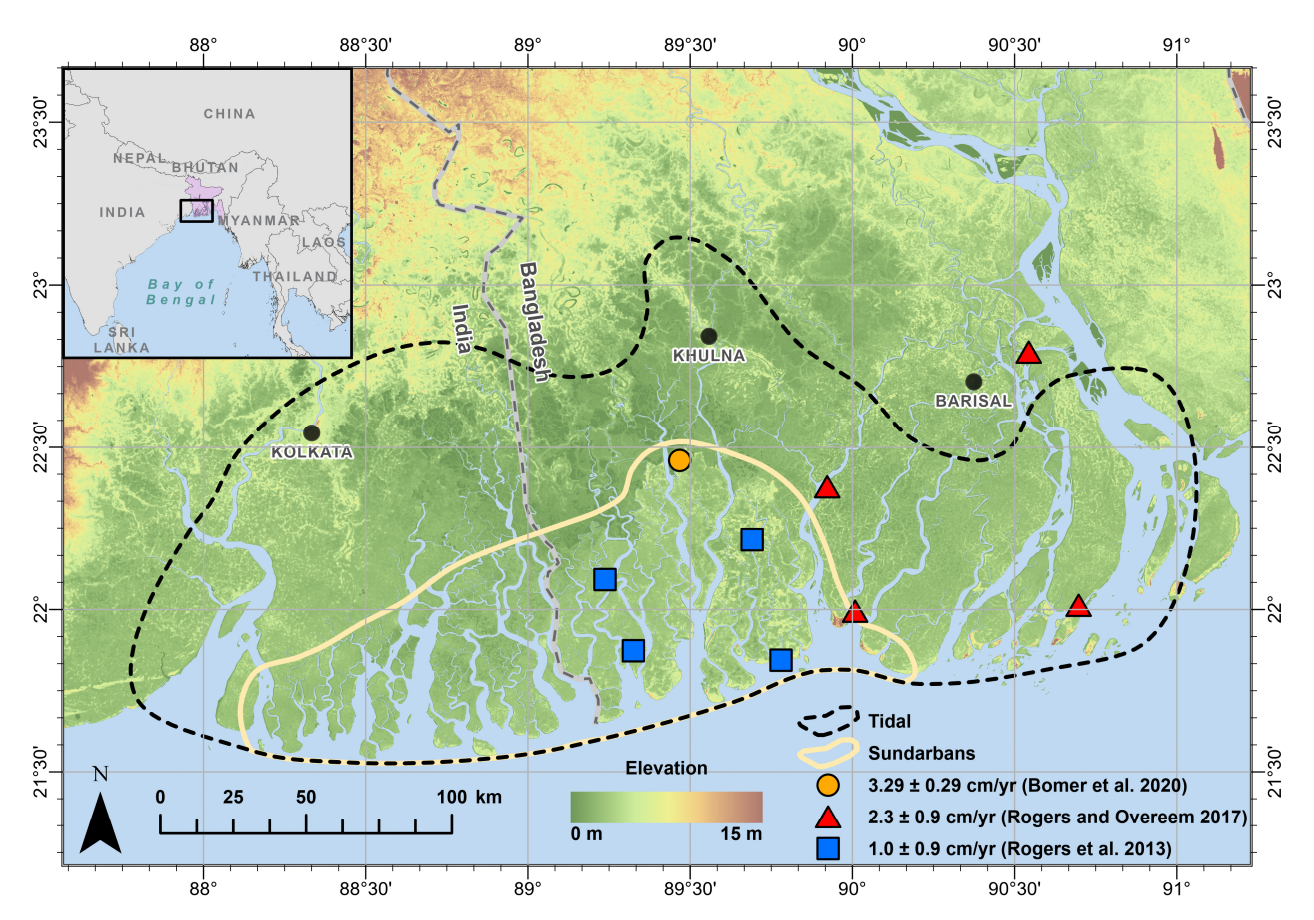


Figure 1: Map of the tide-dominated region of the GBM Delta (black dashed line) and the Sundarbans mangrove forest (light solid line). The inset shows the regional context, and the black square indicates the area shown in the elevation map. Elevation data is from CoastalDEM (Kulp and Strauss 2021). Several studies of sedimentation are indicated on the elevation map.

the South Asian Monsoon, as is expected. This would greatly increase the amount of sediment transported to the coast by the GBM river system. However, Raff et al. (2023) also highlight that upstream damming or river diversions could reduce sediment flux enough to threaten this stability.

Many studies have attempted to quantify changes in sediment load. Darby et al. (2015) suggests it could increase by nearly 50 % in response to increased weathering and erosion. Other studies suggest it may decrease by anywhere from 30 % (Higgins et al. 2018) to 88 % (Dunn et al. 2018) largely in response to upstream damming and land-use changes. SLR is also very uncertain: the IPCC (2021) gives likely ranges from 0.28 to 1.01 m by 2100, with possible extreme values as high as 5 m. This uncertainty makes it important to assess the sustainability of the delta under different conditions.

In order to understand how the system may evolve in the future, we must understand the dynamics that currently control the elevation of the delta. Presently, many studies (Allison and Kepple 2001; Rogers et al. 2013; Bomer et al. 2020a) have shown platform elevations are maintaining pace with SLR. This implies that the mangroves may be incredibly resilient to increasing water levels due, in large part, to the sediment delivered to the platform periodically during high tide. This process enables the mangrove platforms to exist in a dynamic equilibrium approximately between mean high water (MHW) and mean spring high water (MSHW).

Counterintuitively, some studies (Rogers and Overeem 2017; Bomer et al. 2020a; Chaudhuri et al. 2020; Rahman et al. 2022) have shown rates of aggradation that exceed rates of relative sea-level rise (RSLR)

(subsidence and eustatic SLR). Fundamentally, the elevation of a tidal platform is controlled by the available depositional volume or accommodation space. For a point on a tidal platform, this can be simplified as the difference between the elevation of high water (HW) and the elevation of the platform. Thus, the equilibrium elevation of a platform should be approximated by the difference between the terms resulting in positive platform elevation change (aggradation) and negative platform elevation change (subsidence and changes in HW). By this logic, the high rates of aggradation described by these studies may be capturing a transient phenomenon.

Given the wide range of possible future rates of SLR and sediment load, it will be useful to have a simulation model that can assess the combined impact of sediment transport and SLR over time spans of decades or more. In principle, many geomorphological models, such as Delft3D (Deltares 2023), can simulate coastal landscape change under the combined influence of erosion and deposition of sediment, SLR, and other factors, but these require detailed gridded input data on land-surface elevation, channel bathymetry, etc., and are computationally expensive for simulating change on large spatial and temporal scales. Here, we present a much simpler model of elevation change in response to tidal inundation, aggradation, and subsidence. This framework provides a generalizable way of investigating elevation change within a tidal delta at various scales, and with minimal demands for input data. For the purpose of this study, we use the model to investigate (1) the long-term viability of the high rates of aggradation observed throughout the delta and (2) the timescales over which they persist. We do so by modeling the multi-decadal elevation change of a tidal platform near a stream-bank as described by Bomer et al. (2020a). Specifically, we construct a zero-dimensional model of elevation change at a site in Dakop Upazila, in Khulna District, near the confluence of the Sutarkhali and Sorbotkhali Rivers and adjacent to Polder 32 (Figure 1). This area was chosen not only for the high rates of aggradation but also for the availability of data from a plethora of recent studies (Auerbach et al. 2015; Hale et al. 2019a; Hale et al. 2019b; Bomer et al. 2020a; Bomer et al. 2020b; Steckler et al. 2022), which allowed us to calibrate and test our model.

2 METHODS

2.1 Model description

We model the elevation of a tidal platform (η) using a zero-dimensional mass balance approach described by Krone (1987) and refined by subsequent studies (Allen 1990; French 1993; Temmerman et al. 2003; Temmerman et al. 2004). We first conceptualize a periodically inundated tidal platform. The depth of inundation, h, is defined as

$$h(t) = \zeta(t) - \eta(t),$$

where $\zeta(t)$ is the water-surface elevation and $\eta(t)$ is the sediment-surface elevation. The rate of elevation change of the platform is described as

$$\frac{d\eta(t)}{dt} = \frac{dS_m(t)}{dt} + \frac{dS_o(t)}{dt} + \frac{dP(t)}{dt} + \frac{dM(t)}{dt},\tag{1}$$

where $dS_m(t)/dt$ is the rate of mineral sedimentation, $dS_o(t)/dt$ is the rate of organic matter sedimentation, dP(t)/dt is the rate of shallow compaction, and dM(t)/dt is the rate of subsidence due to tectonics and deep compaction. While the platform is inundated (h(t) > 0), the rate of mineral sedimentation is

$$\frac{dS_m(t)}{dt} = \frac{w_s C(t)}{\rho_b},\tag{2}$$

where w_s is the nominal settling velocity of a sediment grain, C(t) is the depth-averaged suspended sediment concentration (SSC) within the water column, and ρ_b is the bulk density of the sediment. We assume no resuspension of sediment which is consistent with previous studies (Krone 1987; Allen 1990; French 1993; Temmerman et al. 2003; Temmerman et al. 2004).

In order to solve for concentration, we define a mass balance of sediment within the water column as

$$\frac{d}{dt}[h(t)C(t)] = -w_sC(t) + C_p\frac{dh(t)}{dt},$$

where C_p is the SSC of the inflowing water from outside the model. This can be rewritten as

$$\frac{dC(t)}{dt} = -\frac{w_s C(t)}{h(t)} - \frac{1}{h(t)} [C(t) - C_p] \frac{dh(t)}{dt}.$$
 (3)

Sediment is only imported to the platform during a flood tide. We impose this condition by only allowing new sediment to enter the model while the water-surface elevation is rising (dh/dt > 0). This is formalized as a Heaviside step function which serves as a switch for the platform concentration and is given as

$$z = \frac{dh}{dt}, \quad H(z) = \begin{cases} 0, & z < 0; \\ 1, & z \ge 0. \end{cases}$$

We also include a term for trapping efficiency (ϕ) to capture the effect of decreased sediment aggradation with increased distance from the tidal channel and thus, define platform concentration as

$$C_p = \phi C_c H(z), \tag{4}$$

where C_c is the average annual SSC of the nearest primary tidal channel. We use ϕ as a tuning parameter which we adjust to ensure modeled rates of sediment aggradation match field observations for a location.

For each time step, we solve equation (3) then equation (2) to find concentration and rate of mineral sedimentation, respectively. These equations are integrated for each inundation period using an explicit 5(4)-order adaptive step-size Runge-Kutta method (Dormand and Prince 1980), implemented in Python using SciPy (Virtanen et al. 2020). To avoid numerical instabilities at very small depths in equation (3), we constrain the model to run only while h > 1 mm. We calculate the sediment-surface elevation before and after each inundation cycle using equation (1).

2.2 Model parameterization and calibration

We parameterized our model using a combination of field observations and estimates from the literature as described below and summarized in Table 1. All elevations are referenced to the EGM96 geoid.

Parameter	Value	Source
Organic matter sedimentation (S_o)	$0.5\mathrm{mm}\mathrm{yr}^{-1}$	Rogers et al. 2013; Bomer et al. 2020b
Compaction (P)	$-11.3\mathrm{mm}\mathrm{yr}^{-1}$	Bomer et al. 2020a
Subsidence (M)	$-2.5\mathrm{mm}\mathrm{yr}^{-1}$	Steckler et al. 2022
Settling velocity (w_s)	$0.5\mathrm{mm}\mathrm{s}^{-1}$	Rogers et al. 2013; Hale et al. 2019b; Bomer et al. 2020b
Dry bulk density (ρ_b)	$1\mathrm{gcm^{-3}}$	Allison and Kepple 2001; Hale et al. 2019b; Bomer et al. 2020b
Tidal channel SSC (C_c)	$0.5{\rm gL^{-1}}$	Hale et al. 2019a

Table 1: Model parameters and sources.

2.2.1 Tides

Our model uses a simulated tide curve for the water-surface elevations (ζ). The tidal data were derived from observations at the dock of the Sutarkhali Forest Ranger Station. Water-surface elevations were collected in 10 min increments from May 18, 2014, to October 2, 2018, using an Onset U20L-01 HOBO water level data logger. The period of record contains many gaps and datum shifts due to expected (periodic data retrieval) and unexpected (instrument failure) causes.

Sufficiently small gaps ($<12\,h$) without datum shifts were interpolated using a cubic spline. Small gaps ($<3\,d$) were corrected by adjusting the right side (later dates) of the gap so that the 14-day medians of each side of the gap were equal. The 14-day median was used to negate the impact of spring-neap cycles. A near year-long gap due to instrument failure was corrected similarly using a 1 yr median on each side of the gap. Lastly, an 81-day gap was adjusted by analyzing the equivalent time period in three other years and shifting the right side of the gap accordingly. Correcting these datum shifts expanded the usable tide record by $\sim40\,\%$ for a total of $\sim4.5\,\mathrm{yr}$.

From the corrected data, we created a model of the tides using the Python implementation of UTide (Codiga 2011) which explicitly allows for gaps and includes the 18.61 yr lunar nodal oscillation. We disabled UTide from fitting a linear trend so that the model produced a general, stationary tidal curve. Finally, using this tidal model, we created a multi-decadal tide curve and superimposed 3 cm yr⁻¹ of SLR which is consistent with recent observations (Pethick and Orford 2013; Becker et al. 2020; Fox-Kemper et al. 2021).

2.2.2 Background rates — organic matter sedimentation, compaction, and subsidence

The sediment of the Sundarbans contains very little organic matter as compared to other mangrove forests. Rogers et al. (2013) found organic content of Sundarbans soils to only accounts for 2.9 to 3.8 % of a total vertical accretion rate of $1.0\pm0.9\,\mathrm{cm}\,\mathrm{yr}^{-1}$. Bomer et al. (2020a) found an average total organic content of $0.9\pm0.1\,\%$ and total vertical accretion rates of $3.29\pm0.24\,\mathrm{cm}\,\mathrm{yr}^{-1}$. Using these estimates, we set S_O to be $0.5\,\mathrm{mm}\,\mathrm{yr}^{-1}$.

Compaction and subsidence are difficult to disentangle. Estimates for the region are often lumped or split in various ways. For our study area, Auerbach et al. (2015) suggested $4.0\pm0.2~\mathrm{mm\,yr^{-1}}$ for compaction and $3.0\pm0.2~\mathrm{mm\,yr^{-1}}$ for subsidence. More recently, Bomer et al. (2020a) observed significantly higher rates of compaction ($11.3\pm0.5~\mathrm{mm\,yr^{-1}}$) using a rod surface elevation table (RSET) and sediment traps. Following on this, Steckler et al. (2022) estimates an additional 2 to $3~\mathrm{mm\,yr^{-1}}$ of deeper subsidence below the base of the RSET. From this, we set compaction and subsidence to $-11.3~\mathrm{mm\,yr^{-1}}$ and $-2.5~\mathrm{mm\,yr^{-1}}$, respectively.

2.2.3 Controls on mineral sedimentation — settling velocity, dry bulk density and SSC

We determine the settling velocity using Stokes' law for a characteristic grain size in our study area. Rogers et al. (2013) observed median grain sizes of $23.5 \pm 4.7 \,\mu m$ for multiple sites in the western Sundarbans. Similarly, within our study area, Bomer et al. (2020b) and Hale et al. (2019a) found median grain sizes of $23.9 \,\mu m$ and $31 \,\mu m$, respectively. We use a grain size of $25 \,\mu m$ (medium silt) and assume a grain density of $2.65 \, g \, cm^{-1}$ (quartz) leading to a settling velocity of $\sim 0.5 \, mm \, s^{-1}$.

Estimates for dry bulk density vary greatly depending on the season and location on the platform. Allison and Kepple (2001) estimated mean bulk density of the upper 1 m of the lower GBM Delta plain to be $1.3\,\mathrm{g\,cm^{-3}}$. Within our study area, both Hale et al. (2019b) and Bomer et al. (2020b) observed densities ranging from 0.6 to $1.1\,\mathrm{g\,cm^{-3}}$. Though, Bomer et al. (2020b) saw some increase in density over the upper $0.5\,\mathrm{m}$. Due to this increase with depth, we set our bulk density toward that higher end of the range at $1\,\mathrm{g\,cm^{-3}}$.

We have limited information for SSC on the platform outside sparse single-day observations by Hale et al. (2019b). However, in a separate study, Hale et al. (2019a) conducted an extensive survey of the main stem tidal channel that feeds this area. They estimated mean annual discharge of the Shibsa River to

be 2×10^{11} m³ and 1×10^{11} kg, respectively, which equates to a mean annual SSC of 0.5 gL⁻¹. From this, we found the platform SSC as a fraction of the tidal channel SSC by applying a trapping efficiency using equation (4).

2.3 Model tuning and execution

We tuned the model to match observed rates of elevation change (2.59 cm yr⁻¹) from Bomer et al. (2020a) over the 5 yr observation period from 2014 to 2019. Since our model considers subsidence, whereas Bomer et al. (2020a) does not, we tuned it to a 5 yr mean elevation change of 2.34 cm yr⁻¹. This step depended greatly on the initial platform elevation relative to the tides. Due to inherent uncertainties in the exact initial elevation, we tuned the model for a range of initial platform elevations. Finally, after we tuned trapping efficiency and found the platform SSC, we ran each simulation from 2014 to 2070.

3 RESULTS

3.1 Model tuning

The tuning processed showed a sublinear relationship between platform SSC and mean elevation change regardless of initial platform elevation. Mean annual elevation change during the 5 yr window diminished at higher values of trapping and SSCs. As an example, Figure 2 shows how we determined the annual mean platform SSC for an initial elevation of 2.5 m. For this initial elevation, a trapping efficiency of 0.83 and platform SSC of $0.41\,\mathrm{g\,L^{-1}}$ were required to obtain the target elevation change of $2.34\,\mathrm{cm\,yr^{-1}}$. In other words, if the platform observed by Bomer et al. (2020a) started at an elevation of $2.5\,\mathrm{m}$, a platform SSC equivalent to $83\,\%$ of the annual tidal channel SSC ($0.5\,\mathrm{g\,L^{-1}}$) is required.

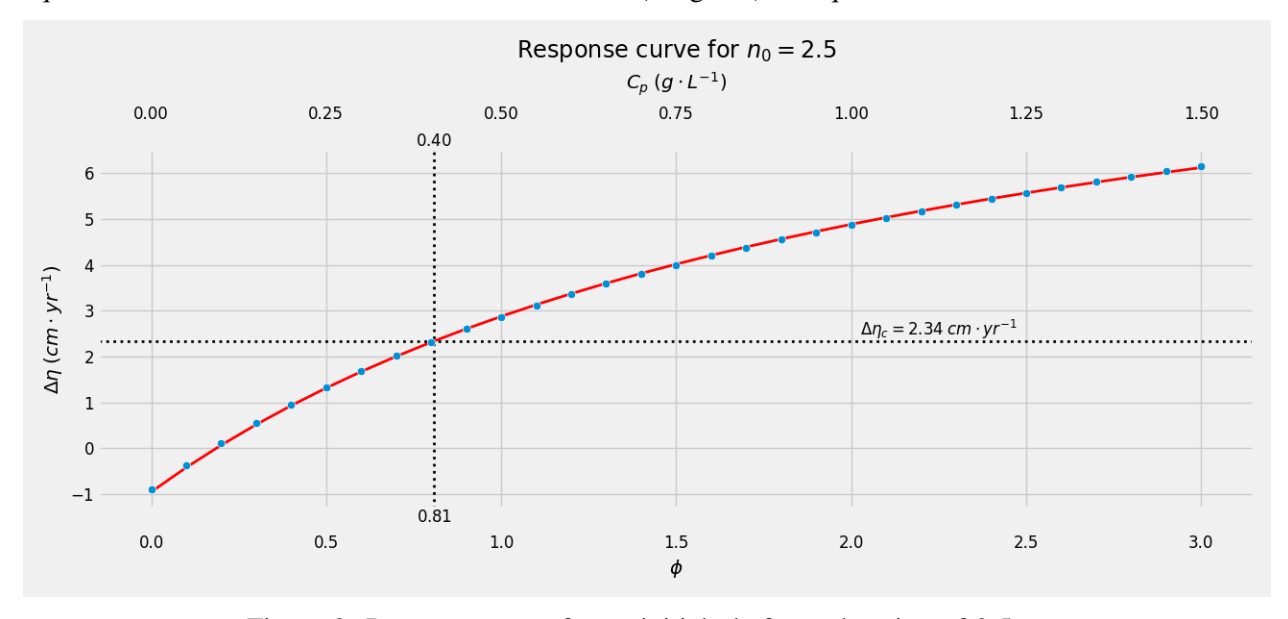


Figure 2: Response curve for an initial platform elevation of 2.5 m.

Expanding on this, we found the required trapping efficiency and platform SSC for other initial elevations which led to the curve shown in Figure 3. This curve shows the required trapping efficiency and platform SSC for any initial platform elevation. Trapping efficiency had a positive exponential relationship with the initial platform elevation. A trapping efficiency of one indicates that the mean annual SSC of the tidal channel and platform are equal.

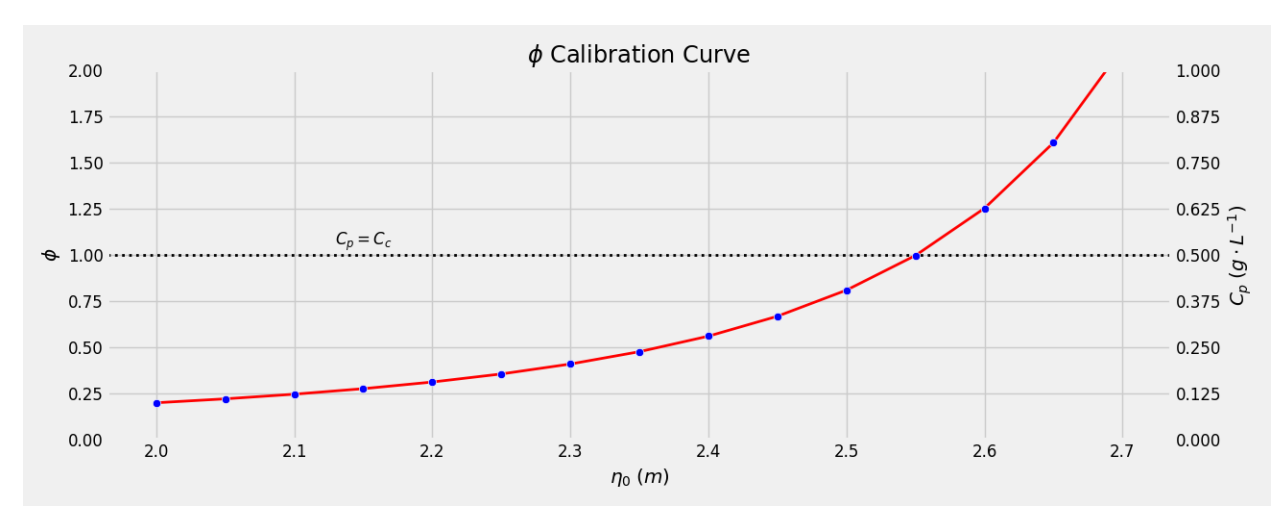


Figure 3: Rating curve showing the required trapping efficiency and platform SSC for a given initial elevation.

3.2 Multi-decadal simulations of tidal platform elevation

We simulated the evolution of a tidal platform across a range of initial elevations from 2.1 to 2.65 m. The elevation of all simulations started at or below MHW. The median simulation increased quickly during the first 25 yr, after which, it was roughly in equilibrium with 3 mm of SLR. The other simulations followed similarly and by the end of the simulation period all were in equilibrium between MHW and MSHW.

The rate of elevation change quickly declined below the 5 yr average rate from Bomer et al. (2020a) (dotted line in Figure 4b) for all simulations. Each simulation crossed the $2.34 \, \mathrm{cm} \, \mathrm{yr}^{-1}$ target at exactly 2.5 yr (half of the tuning window) which is an effect of the tuning process. Interestingly, this is also the point at which the simulation with the lowest initial elevation overtook the one with the highest initial elevation. Within 15 yr, the rate of elevation change of the median simulation was less than half the observed rates of Bomer et al. (2020a) and within $\sim 20 \, \mathrm{yr}$, all simulations were below this mark. By the end of the simulation period, the variation between the simulations was negligible.

The mean hydroperiod started relatively high with the median simulation being inundated on average for \sim 2.95 h. However, similar to previous metrics, this quickly tailed to an apparent equilibrium within 25 yr. By 2040, most simulations equilibrated to a mean hydroperiod between 2.0 to 2.8 h, with the median simulation having a mean hydroperiod of \sim 2.5 h.

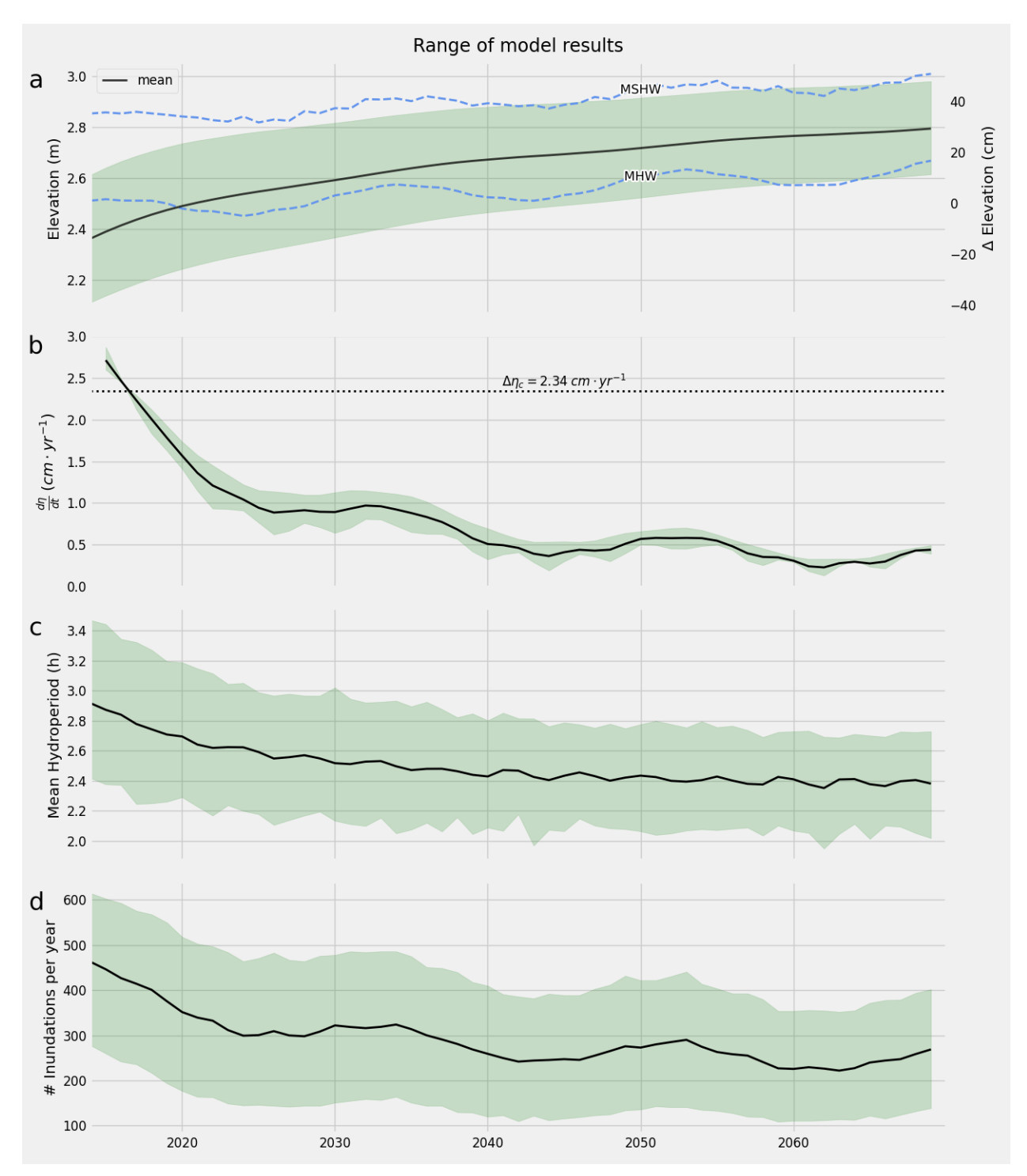


Figure 4: Simulation results from 2014 to 2070. The solid line shows the median simulation result and the shading shows the range of simulation results. Panel (a) shows platform elevation referenced to EGM96 (left axis) and relative elevation change (right axis). Panel (b) shows the rate of elevation change of the platform. Panel (c) shows the mean hydroperiod of an inundation event. Panel (d) shows the number of times per year that the platform is submerged by tides.

4 DISCUSSION

Our analysis reveals discrepancies between simulated and observed rates of aggradation in the Shibsa River. The simulation results (Figure 4) shows that the rates of aggradation observed by Bomer et al. (2020a) are not sustainable over multi-decadal timescales. Indeed, Bomer et al. (2020a) noted that these rates of aggradation exceeded RSLR for the region and suggested that this may be due to an external forcing like tidal amplification.

Further, an initial platform elevation above 2.55 m is not plausible as this would imply that the water inundating the platform would have a greater SSC than the river (Figure 3). However, many other studies (Auerbach et al. 2015; Hale et al. 2019b; Bomer et al. 2020b) have reported similar platform elevation in this region, between 2.55 to 2.65 m. Thus, we similarly conclude that the observed sustained rates of aggradation are implausible without additional forcings.

The elevation of a platform is in static equilibrium when aggradation and subsidence are equal. Assuming a constant sediment supply, a steady state elevation in the presence of an external forcing, such as SLR, should respond by increasing aggradation to match the combined rates of subsidence and SLR. However, the observed rates of aggradation exceed subsidence and SLR by an order of magnitude. This implies that there is a significant disequilibrium, additional forcings are contributing, or there is a more complicated dynamic equilibrium between SLR, tidal range, and platform elevation.

4.1 Platform elevation (dis)equilibrium and potential explanations

The simplest potential explanation for this discrepancy would be that the actual SSC at our study area is significantly greater than the value in Table 1, which was extrapolated from coarse estimates of SSC in the main stem tidal channel downstream from our study area. We do not have measurements that could provide the mean annual SSC at the study site, either in the tidal channel or on the inundated platform. We address this by assuming that SSC on the platform is proportional to the SSC measured downstream in the Shibsa River. However, the tidal network is known to be complex (Bain et al. 2019; Bain 2019; Hale et al. 2019a), so there could be important spatial and temporal variations in SSC. For instance, Hale et al. (2019a) reported asymmetries between the ebb and flood tidal prism near our study area, which they attribute to a lateral (east-west) transfer of water between the Shibsa River and the adjacent main stem tidal channel (Pasur River) to the east, which implies that sediment in our study area may be sourced from both rivers. However, both rivers likely carry similar sediment loads (Hale et al. 2019a), so it seems unlikely that this could explain the discrepancy in aggradation rates.

Another potential explanation is that total rate of compaction and deep subsidence exceeds the estimate in Table 1. Compaction is unlikely to be significantly different from our estimates because Bomer et al. (2020a) report measured compaction at our study location, which is consistent with our estimate. Deep subsidence is more difficult to constrain on a local scale, but an extensive review by Steckler et al. (2022) found consistent measurements of sub-centimeter rates of annual subsidence across the GBM Delta. Thus, it is unlikely that the observed disequilibrium between aggradation and subsidence can be explained by errors in our estimates of compaction and deep subsidence.

A third possible explanation is the lunar nodal cycle, which changes the tidal amplitude over a period of 18.61 yr, and has the effect of stretching the high and low tidal excursions. The 5 yr period observed by Bomer et al. (2020a) occurred during the lead-up to a peak in this cycle (October 2018). Our analysis (Figure 4) found that this cycle increased MHW by \sim 1 cm which is a similar scale to the discrepancy between aggradation and subsidence.

Finally, the tides themselves are nonstationary. Pethick and Orford (2013) speculated that polder construction altered the tidal prism and altered the inland propagation of tides. Analyzing historical tidal records, they found tidal amplification throughout the region, and that at the Port of Mongla, close to our study site, MHW rose by 15 mmyr⁻¹ from 1998 to 2010. This is different from SLR because tidal amplification raises high water and lowers low water. Subsequently, van Maren et al. (2023) found that

this amplification has continued through 2020. Whether instantaneous or sustained, tidal amplification is on a similar order of magnitude as the discrepancy and likely substantially contributes to aggradation.

Future work will incorporate a more thorough treatment of the lunar nodal cycle and tidal amplification and their contribution to driving aggradation. At this time, we are moderately confident that these tidal factors explain the discrepancy.

4.2 Summary

We found that our model could be tuned to match recently observed rates of aggradation using a single tuning parameter to represent sediment trapping efficiency. We found discrepancies between predicted and observed aggradation rates. A more detailed consideration of the tidal prism, which drives aggradation, might explain these differences. Notably, the scale of these discrepancies aligns with the known lunar nodal cycle and observed rates of tidal amplification, bolstering our confidence that these factors likely account for the observed differences.

Aggradation depends on the initial platform elevation, so perturbed landscapes will respond differently than natural ones, such as the relatively undisturbed mangrove forest. Our simulations produce aggradation rates that can easily compensate for 5 mm yr⁻¹ of SLR, maintaining equilibrium between the land and sea level. Greater inundation depths and hydroperiods produce faster aggradation, which suggests that so long as SSCs remain near current levels, aggradation should be able to compensate for even greater rates of SLR. Climate change is likely to strengthen the South Asian Monsoon, which is predicted to increase sediment discharge from the GBM river system by 34 to 60 % (Darby et al. 2015; Raff et al. 2023). This strengthens the prospect that natural sediment transport has great potential to protect the GBM Delta from SLR.

Although our simplified approach to simulating the evolution of the coastal zone of the GBM Delta cannot predict the details of local variation in landscape change across the delta, it offers insights into the general dynamics of the deltaic system as a whole. We conclude that under current conditions of sediment supply and tidal range, this tidal platform system is in not in a static equilibrium with the tides, but may either be subject to a more complex dynamic equilibrium with changing tides, or alternatively, may simply be re-equilibrating to a recent disturbance, such as the massive coastal-embankment project. Future work will apply the modeling tool described here to investigate these alternatives.

Full code and documentation for the model described here are available at github.com/christasich/tidal_flat.

ACKNOWLEDGEMENTS

This work was supported by the National Science Foundation grants Coastal SEES 1600319 and CNH 1716909 and by Vanderbilt University's Grand Challenge Initiative on Climate and Society. The authors thank Rachel Bain, Tyler Doane, David Furbish, Steve Goodbred, Irina Overeem, Chelsea Peters, Jessica Raff, Matt Dietrich, Kimberly Rogers, Leslie Valentine, and Carol Wilson for helpful discussions.

REFERENCES

- Alam, M. S., N. Sasaki, and A. Datta. 2017, September. "Waterlogging, Crop Damage and Adaptation Interventions in the Coastal Region of Bangladesh: A Perception Analysis of Local People". *Environmental Development* 23:22–32.
- Allen, J. 1990, November. "Salt-Marsh Growth and Stratification: A Numerical Model with Special Reference to the Severn Estuary, Southwest Britain". *Marine Geology* 95(2):77–96.
- Allison, M., and E. Kepple. 2001, September. "Modern Sediment Supply to the Lower Delta Plain of the Ganges-Brahmaputra River in Bangladesh". *Geo-Marine Letters* 21(2):66–74.
- Auerbach, L. W., S. L. Goodbred Jr, D. R. Mondal, C. A. Wilson, K. R. Ahmed, K. Roy, M. S. Steckler, C. Small, J. M. Gilligan, and B. A. Ackerly. 2015, February. "Flood Risk of Natural and Embanked Landscapes on the Ganges–Brahmaputra Tidal Delta Plain". *Nature Climate Change* 5(2):153–157.
- Bain, R. L. 2019, November. *Tidal Hydrodynamics in the Interconnected Channel Network of the Southwestern Ganges-Brahmaputra-Meghna Delta, Bangladesh.* Ph. D. thesis, Vanderbilt University.

Tasich, Gilligan, and Hornberger

- Bain, R. L., R. P. Hale, and S. L. Goodbred. 2019, August. "Flow Reorganization in an Anthropogenically Modified Tidal Channel Network: An Example From the Southwestern Ganges-Brahmaputra-Meghna Delta". *Journal of Geophysical Research: Earth Surface* 124(8):2141–2159.
- Becker, M., F. Papa, M. Karpytchev, C. Delebecque, Y. Krien, J. U. Khan, V. Ballu, F. Durand, G. Le Cozannet, A. K. M. S. Islam, S. Calmant, and C. K. Shum. 2020, January. "Water Level Changes, Subsidence, and Sea Level Rise in the Ganges-Brahmaputra-Meghna Delta". Proceedings of the National Academy of Sciences 117(4):1867–1876.
- Bomer, E. J., C. A. Wilson, and T. Elsey-Quirk. 2020b, July. "Process Controls of the Live Root Zone and Carbon Sequestration Capacity of the Sundarbans Mangrove Forest, Bangladesh". *Sci* 2(3):54.
- Bomer, E. J., C. A. Wilson, R. P. Hale, A. N. M. Hossain, and F. A. Rahman. 2020a, April. "Surface Elevation and Sedimentation Dynamics in the Ganges-Brahmaputra Tidal Delta Plain, Bangladesh: Evidence for Mangrove Adaptation to Human-Induced Tidal Amplification". *CATENA* 187:104312.
- Brammer, H. 2014. "Bangladesh's Dynamic Coastal Regions and Sea-Level Rise". Climate Risk Management 1:51-62.
- Chaudhuri, S., P. Chaudhuri, R. Ghosh, S. Chaudhuri, P. Chaudhuri, and R. Ghosh. 2020, October. "The Impact of Embankments on the Geomorphic and Ecological Evolution of the Deltaic Landscape of the Indo-Bangladesh Sundarbans". In *River Deltas Research Recent Advances*, edited by Andrew J. Manning. IntechOpen.
- Codiga, D. 2011, September. "Unified Tidal Analysis and Prediction Using the UTide Matlab Functions". Technical Report, Graduate School of Oceanography, University of Rhode Island, Narragansett, RI.
- Darby, S. E., F. E. Dunn, R. J. Nicholls, M. Rahman, and L. Riddy. 2015. "A First Look at the Influence of Anthropogenic Climate Change on the Future Delivery of Fluvial Sediment to the Ganges–Brahmaputra–Meghna Delta". *Environmental Science: Processes & Impacts* 17(9):1587–1600.
- Dasgupta, S., B. Laplante, C. Meisner, D. Wheeler, and J. Yan. 2009, April. "The Impact of Sea Level Rise on Developing Countries: A Comparative Analysis". *Climatic Change* 93(3-4):379–388.
- Deltares 2023. Delft3D-FLOW User Manual. Delft, NL: Deltares.
- Dormand, J., and P. Prince. 1980, March. "A Family of Embedded Runge-Kutta Formulae". *Journal of Computational and Applied Mathematics* 6(1):19–26.
- Dunn, F. E., R. J. Nicholls, S. E. Darby, S. Cohen, C. Zarfl, and B. M. Fekete. 2018, November. "Projections of Historical and 21st Century Fluvial Sediment Delivery to the Ganges-Brahmaputra-Meghna, Mahanadi, and Volta Deltas". *Science of The Total Environment* 642:105–116.
- Fox-Kemper, B., H. T. Hewitt, C. Xiao, G. Aðalgeirsdóttir, S. S. Drijfhout, T. L. Edwards, N. R. Golledge, M. Hemer, R. E. Kopp, G. Krinner, A. Mix, D. Notz, S. Nowicki, I. S. Nurhati, L. Ruiz, J.-B. Sallée, A. B. A. Slangen, and Y. Yu. 2021. "Ocean, Cryosphere, and Sea Level Change". In *Climate Change 2021: The Physical Science Basis. Contribution of Working Group I to the Sixth Assessment Report of the Intergovernmental Panel on Climate Change*, edited by V. Masson-Delmotte, P. Zhai, A. Pirani, S. L. Connors, C. Péan, S. Berger, N. Caud, Y. Chen, L. Goldfarb, M. I. Gomis, M. Huang, K. Leitzell, E. Lonnoy, J. B. R. Matthews, T. K. Maycock, T. Waterfield, Ö. Yelekçi, R. Yu, and B. Zhou. Cambridge University Press.
- French, J. R. 1993, February. "Numerical Simulation of Vertical Marsh Growth and Adjustment to Accelerated Sea-Level Rise, North Norfolk, U.K.". Earth Surface Processes and Landforms 18(1):63-81.
- Hale, R., R. Bain, S. Goodbred Jr., and J. Best. 2019a, March. "Observations and Scaling of Tidal Mass Transport across the Lower Ganges-Brahmaputra Delta Plain: Implications for Delta Management and Sustainability". Earth Surface Dynamics 7(1):231–245.
- Hale, R. P., C. A. Wilson, and E. J. Bomer. 2019b, August. "Seasonal Variability of Forces Controlling Sedimentation in the Sundarbans National Forest, Bangladesh". Frontiers in Earth Science 7:211.
- Higgins, S. A., I. Overeem, K. G. Rogers, and E. A. Kalina. 2018, January. "River Linking in India: Downstream Impacts on Water Discharge and Suspended Sediment Transport to Deltas". *Elementa: Science of the Anthropocene* 6(1):20.
- IPCC 2021. Climate Change 2021: The Physical Science Basis. Contribution of Working Group I to the Sixth Assessment Report of the Intergovernmental Panel on Climate Change, Volume In Press. Cambridge, United Kingdom and New York, NY, USA: Cambridge University Press.
- Krone, R. 1987. "A Method for Simulating Marsh Elevations". In *Coastal Sediments*, 316–323. New Orleans, Louisiana: American Society of Civil Engineers.
- Kulp, S. A., and B. H. Strauss. 2021. "CoastalDEM v2.1: A High-Accuracy and High-Resolution Global Coastal Elevation Model Trained on ICESat-2 Satellite Lidar". *Climate Central* 17.
- Loucks, C., S. Barber-Meyer, M. A. A. Hossain, A. Barlow, and R. M. Chowdhury. 2010, January. "Sea Level Rise and Tigers: Predicted Impacts to Bangladesh's Sundarbans Mangroves: A Letter". *Climatic Change* 98(1-2):291–298.
- Pethick, J., and J. D. Orford. 2013, December. "Rapid Rise in Effective Sea-Level in Southwest Bangladesh: Its Causes and Contemporary Rates". *Global and Planetary Change* 111:237–245.
- Raff, J. L., S. L. Goodbred, J. L. Pickering, R. S. Sincavage, J. C. Ayers, M. S. Hossain, C. A. Wilson, C. Paola, M. S. Steckler, D. R. Mondal, J.-L. Grimaud, C. J. Grall, K. G. Rogers, K. M. Ahmed, S. H. Akhter, B. N. Carlson, E. L. Chamberlain, M. Dejter, J. M. Gilligan, R. P. Hale, M. R. Khan, M. G. Muktadir, M. M. Rahman, and L. A. Williams.

Tasich, Gilligan, and Hornberger

- 2023, April. "Sediment Delivery to Sustain the Ganges-Brahmaputra Delta under Climate Change and Anthropogenic Impacts". *Nature Communications* 14(1):2429.
- Rahman, M. M., A. Haque, R. J. Nicholls, S. E. Darby, M. T. Urmi, M. M. Dustegir, F. E. Dunn, A. Tahsin, S. Razzaque, K. Horsburgh, and M. A. Haque. 2022, July. "Sustainability of the Coastal Zone of the Ganges-Brahmaputra-Meghna Delta under Climatic and Anthropogenic Stresses". *Science of The Total Environment* 829:154547.
- Rogers, K. G., S. L. Goodbred, and D. R. Mondal. 2013, October. "Monsoon Sedimentation on the 'Abandoned' Tide-Influenced Ganges-Brahmaputra Delta Plain". *Estuarine, Coastal and Shelf Science* 131:297–309.
- Rogers, K. G., and I. Overeem. 2017, January. "Doomed to Drown? Sediment Dynamics in the Human-Controlled Floodplains of the Active Bengal Delta". *Elementa: Science of the Anthropocene* 5:66.
- Roy, K., A. K. Gain, B. Mallick, and J. Vogt. 2017, October. "Social, Hydro-Ecological and Climatic Change in the Southwest Coastal Region of Bangladesh". *Regional Environmental Change* 17(7):1895–1906.
- Sarwar, M. G. M. 2005, November. "Impacts of Sea Level Rise on the Coastal Zone of Bangladesh". Master's thesis, Lund University.
- Steckler, M. S., B. Oryan, C. A. Wilson, C. Grall, S. L. Nooner, D. R. Mondal, S. H. Akhter, S. DeWolf, and S. L. Goodbred. 2022, January. "Synthesis of the Distribution of Subsidence of the Lower Ganges-Brahmaputra Delta, Bangladesh". *Earth-Science Reviews* 224:103887.
- Temmerman, S., G. Govers, P. Meire, and S. Wartel. 2003, January. "Modelling Long-Term Tidal Marsh Growth under Changing Tidal Conditions and Suspended Sediment Concentrations, Scheldt Estuary, Belgium". *Marine Geology* 193(1-2):151–169.
- Temmerman, S., G. Govers, S. Wartel, and P. Meire. 2004, November. "Modelling Estuarine Variations in Tidal Marsh Sedimentation: Response to Changing Sea Level and Suspended Sediment Concentrations". *Marine Geology* 212(1-4):1–19.
- van Maren, D., J. Beemster, Z. Wang, Z. Khan, R. Schrijvershof, and A. Hoitink. 2023, January. "Tidal Amplification and River Capture in Response to Land Reclamation in the Ganges-Brahmaputra Delta". *CATENA* 220:106651.
- Virtanen, P., R. Gommers, T. E. Oliphant, M. Haberland, T. Reddy, D. Cournapeau, E. Burovski, P. Peterson, W. Weckesser, J. Bright, S. J. van Der Walt, M. Brett, J. Wilson, K. J. Millman, N. Mayorov, A. R. J. Nelson, E. Jones, R. Kern, E. Larson, C. J. Carey, İ. Polat, Y. Feng, E. W. Moore, J. VanderPlas, D. Laxalde, J. Perktold, R. Cimrman, I. Henriksen, E. A. Quintero, C. R. Harris, A. M. Archibald, A. H. Ribeiro, F. Pedregosa, P. van Mulbregt, SciPy 1.0 Contributors, A. Vijaykumar, A. P. Bardelli, A. Rothberg, A. Hilboll, A. Kloeckner, A. Scopatz, A. Lee, A. Rokem, C. N. Woods, C. Fulton, C. Masson, C. Häggström, C. Fitzgerald, D. A. Nicholson, D. R. Hagen, D. V. Pasechnik, E. Olivetti, E. Martin, E. Wieser, F. Silva, F. Lenders, F. Wilhelm, G. Young, G. A. Price, G.-L. Ingold, G. E. Allen, G. R. Lee, H. Audren, I. Probst, J. P. Dietrich, J. Silterra, J. T. Webber, J. Slavič, J. Nothman, J. Buchner, J. Kulick, J. L. Schönberger, J. V. De Miranda Cardoso, J. Reimer, J. Harrington, J. L. C. Rodríguez, J. Nunez-Iglesias, J. Kuczynski, K. Tritz, M. Thoma, M. Newville, M. Kümmerer, M. Bolingbroke, M. Tartre, M. Pak, N. J. Smith, N. Nowaczyk, N. Shebanov, O. Pavlyk, P. A. Brodtkorb, P. Lee, R. T. McGibbon, R. Feldbauer, S. Lewis, S. Tygier, S. Sievert, S. Vigna, S. Peterson, S. More, T. Pudlik, T. Oshima, T. J. Pingel, T. P. Robitaille, T. Spura, T. R. Jones, T. Cera, T. Leslie, T. Zito, T. Krauss, U. Upadhyay, Y. O. Halchenko, and Y. Vázquez-Baeza. 2020, March. "SciPy 1.0: Fundamental Algorithms for Scientific Computing in Python". Nature Methods 17(3):261–272.
- Wilson, C., S. Goodbred, C. Small, J. Gilligan, S. Sams, B. Mallick, and R. Hale. 2017, January. "Widespread Infilling of Tidal Channels and Navigable Waterways in the Human-Modified Tidal Deltaplain of Southwest Bangladesh". *Elementa: Science of the Anthropocene* 5:78.

AUTHOR BIOGRAPHIES

Christopher M. Tasich received his a Ph.D. in Environmental Engineering from Vanderbilt University. His research focuses on coastal resilience, tidal dynamics, and sediment transport using numerical models. His email address is christasich@vanderbilt.edu and his website is www.christasich.com.

Jonathan M. Gilligan is Associate Professor of Earth and Environmental Sciences and Civil & Environmental Engineering at Vanderbilt University and director of Vanderbilt's Grand Challenge Initiative on Climate and Society. Their research integrates natural science, social science, and engineering to study sustainability in coupled human-natural systems. They hold a Ph.D. in Physics from Yale University. Their email address is jonathan.gilligan@vanderbilt.edu, their website is www.jonathangilligan.org, and their Twitter handle is @jg_environ.

George M. Hornberger is Professor Emeritus of Civil & Environmental Engineering and Earth & Environmental Sciences at Vanderbilt University. His research interests include hydrology and the Food-Energy-Water Nexus. He holds a Ph.D. in Hydrology from Stanford University. His email address is george.m.hornberger@vanderbilt.edu and his website is www.vanderbilt.edu/viee/profiles/hornberger.php.